Eg5 is static in bipolar spindles relative to tubulin: evidence for a static spindle matrix

Tarun M. Kapoor[1] and Timothy J. Mitchison[2]

[1]Laboratory of Chemistry and Cell Biology, Rockefeller University, New York, NY 10021
[2]Department of Cell Biology, Harvard Medical School, Boston, MA 02115

We used fluorescent speckle microscopy to probe the dynamics of the mitotic kinesin Eg5 in *Xenopus* extract spindles, and compared them to microtubule dynamics. We found significant populations of Eg5 that were static over several seconds while microtubules flux towards spindle poles. Eg5 dynamics are frozen by adenylimidodiphosphate. Bulk turnover experiments showed that Eg5 can exchange between the spindle and the extract with a half life of <55 s. Eg5 distribution in spindles was not perturbed by inhibition of its motor activity with monastrol, but was perturbed by inhibition of dynactin with p50 dynamitin. We interpret these data as revealing the existence of a static spindle matrix that promotes Eg5 targeting to spindles, and transient immobilization of Eg5 within spindles. We discuss alternative interpretations of the Eg5 dynamics we observe, ideas for the biochemical nature of a spindle matrix, and implications for Eg5 function.

Introduction

The mitotic spindle is a transient organizational state of the microtubule cytoskeleton whose dynamic properties are essential for chromosome segregation (for reviews see Nicklas, 1988; Inoue and Salmon, 1995; Wittmann et al., 2001). Microtubule dynamics in spindles are dominated by two processes, rapid turnover by dynamic instability (Mitchison and Kirschner, 1984) and constant movement towards the spindle poles, called polewards flux or treadmilling (Mitchison, 1989). The dynamic behavior of other spindle components is largely unknown. Probing the dynamic behavior of spindle components might shed light on the specific component, and also on the more general question of how the spindle is organized. For example, a key question is whether microtubules alone govern the mechanical and dynamic properties of spindles, or if a second mechanical ensemble exists. If a second ensemble exists, one diagnostic for it would be its effect on the dynamic behavior of spindle components.

A nonmicrotubule "spindle matrix" was first hypothesized to provide an anchor for motor proteins that exert force on microtubules (for reviews see McIntosh et al., 1969; Pickett-Heaps et al., 1982, 1984). Support for the existence of a matrix came from several lines of experiment: extraction of microtubules from isolated spindles produces a "spindle remnant" that retains a spindle shape and contains kinesin and other nonmicrotubule spindle components (Mazia, 1961; Salmon and Segall, 1980; Leslie et al., 1987). Observations of polewards movement of chromosomes with severed kinetochore microtubule bundles (Forer et al., 1997) and the behavior of spindles in which motor proteins were disrupted (Gordon et al., 2001) can be interpreted as providing evidence for a matrix. Recently, the *Drosophila* protein Skeletor was suggested to be a component of a spindle matrix on the basis of its immunolocalization (Walker et al., 2000). This body of evidence is intriguing rather than compelling, and a matrix that permeates the whole spindle has not been directly observed or biochemically characterized. This is in contrast to the spindle pole, where biochemical and imaging evidence supports the idea that NuMA serves as a matrix component (Dionne et al., 1999; Merdes et al., 2000; Gordon et al., 2001) and the centrosome, where pericentrin and related proteins may serve a matrix function (Schnackenberg et al., 1998). Most recent authors have tried to account for spindle dynamics and mechanics in terms of models based purely on microtubules and motor proteins (Sharp et al., 2000). If the matrix hypothesis were correct, such models would require revision.

The mitotic kinesin Eg5 is a conserved spindle component with a key role in establishing bipolar organization of the spindle (Enos and Morris, 1990; Hagan and Yanagida, 1990; Hoyt et al., 1992; Sawin et al., 1992; Heck et al.,

---

Figure 1. **Characterization of recombinant Eg5.** (a) A chromatograph for the purification by gel filtration of labeled full length Eg5 eluted from nickel charged resin. The absorbance at 280 nm (total protein, blue trace) and 590 nm (Texas red, brown trace) wavelengths of light are shown. Standards with Stokes radii 8.5 and 6.1 nm elute at volumes indicated by arrows, s1 and s2, respectively. (b) Coomassie-stained, labeled full-length Eg5 from the fraction corresponding to the major peak (13.5-nm Stokes radius) by gel filtration chromatography is resolved by SDS-PAGE. Protein from this fraction was directly used in the microscopy experiments. (c) In vitro microtubule gliding velocities of labeled and unlabeled Eg5 in 1 mM ATP. Motility assays were performed as described (Mayer et al., 1999). (d) A spindle prepared for fluorescent speckle microscopy of labeled Eg5 (green). Alexa 488–labeled tubulin and Hoechst were added to the extract to visualize the microtubules (red) and DNA (blue). Fig. 2 c shows the distribution of Eg5 alone in this spindle and Fig. 7 a provides a line scan across the image showing the distribution of Eg5 in the spindle relative to microtubules. Bar, 5 μm.
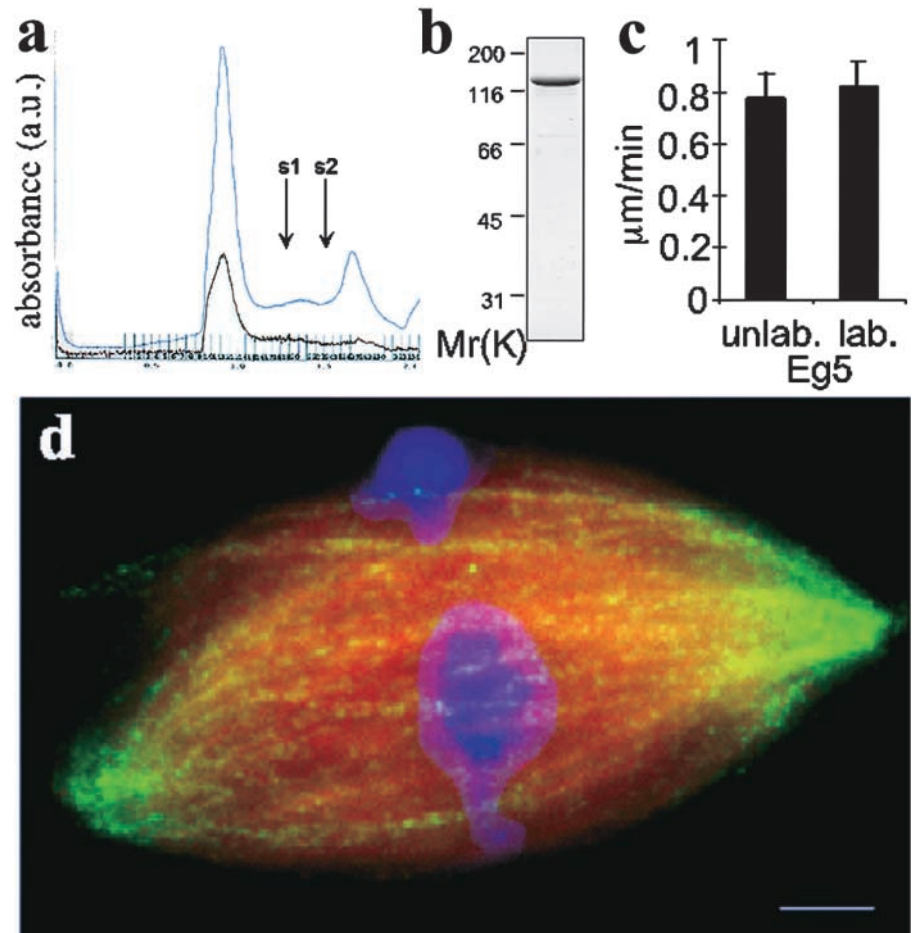
1993; Blangy et al., 1995). In vertebrate somatic cells and *Xenopus* extract spindles, Eg5 is present throughout the spindle, but enriched at the poles relative to microtubules (Sawin and Mitchison, 1995; Kapoor et al., 2000). This unexpected localization for a plus end–directed motor lead to the proposal that Eg5 might target to spindles in part by interacting with some unknown matrix component (Sawin et al., 1992). However, the observation that native Eg5 is a bipolar tetramer lead to an alternative proposal, that Eg5 targets to spindles by binding to two microtubules and cross bridging them, without interacting with other components (Sharp et al., 1999). We know that Eg5 must be phosphorylated on a cdc2 consensus site to target to spindles (Blangy et al., 1995; Sawin and Mitchison, 1995), and two-hybrid experiments suggested that it interacts with the dynactin complex (Blangy et al., 1997). However, the mechanism by which Eg5 targets to spindles, and exactly how it promotes bipolarity, are unresolved.
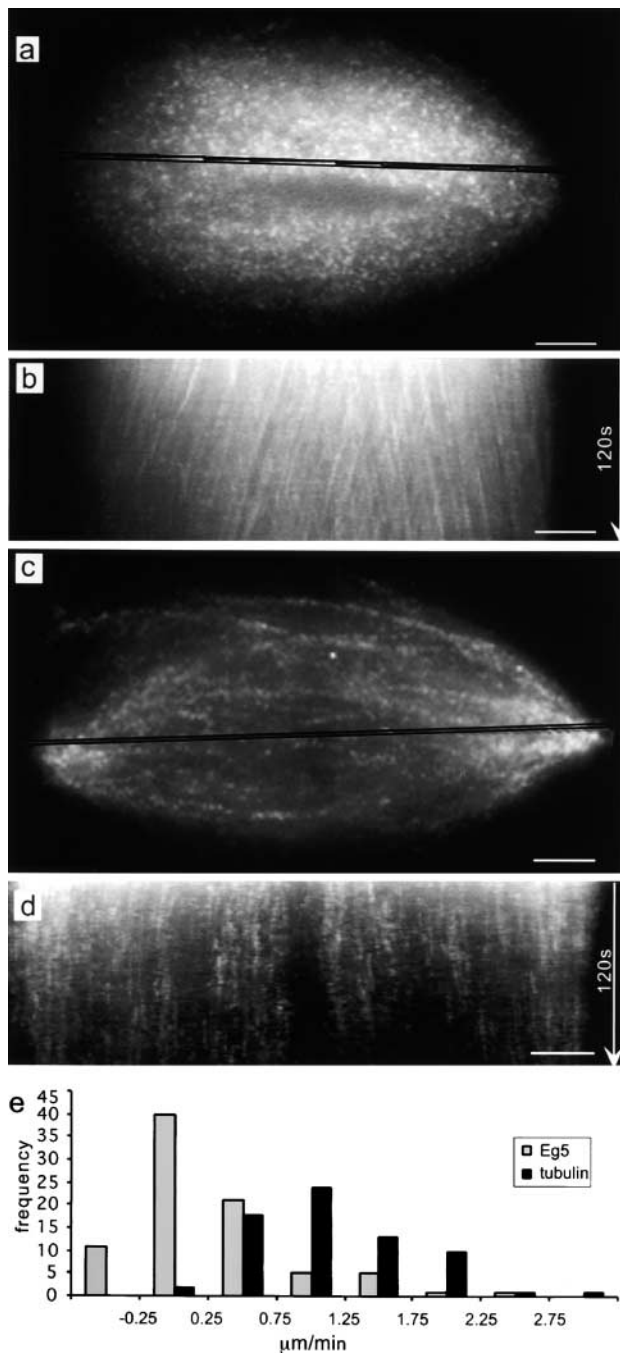
To probe Eg5 dynamics in *Xenopus* extract spindles, and thus gain insight into its targeting mechanism, we sought an imaging method that would provide some sense of its turnover behavior, but more important, would allow us to measure possible translocation of Eg5 along the spindle axis. Recently, fluorescent speckle microscopy has been described as a simple, nonperturbing method for obtaining high-resolution views of microtubule translocation in spindles (Waterman-Storer et al., 1998; Maddox et al., 2000). The speckled image results from stochastic variation in the number of flu-

orophores within minimal regions resolvable by light microscopy. Speckles serve as fiduciary marks, allowing measurement of microtubule movement and turnover (Waterman-Storer and Salmon, 1998). Fluorescent speckle microscopy provides a simple and reliable method for detecting slow, directed movements of immobilized fluorochromes, even in the presence of competing turnover or diffusion. It is more sensitive than either photobleaching or photoactivation for detecting movement in the face of turnover, and thus was our method of choice for parallel analysis of Eg5 and tubulin dynamics. Using this method, we found that although Eg5 can exchange between spindles, within the spindle it is relatively static, whereas microtubules flux poleward. We interpret our observations as revealing the existence of a static, nonmicrotubule mechanical scaffold that influences Eg5 dynamics and may play a central role in spindle organization.

Results

Recombinant Eg5 covalently labeled with a fluorochrome is a functional mitotic motor protein

To make an Eg5 probe for fluorescent speckle microscopy, we expressed and purified full length *Xenopus* laevis Eg5 using a baculovirus system and covalently labeled it with an N-hydroxysuccinimide ester derivative of Texas red (Fig. 1, a and b). The average labeling stochiometry was estimated as 0.5 per polypeptide, or 2 per tetramer. Both the labeled and

Figure 2.   **Comparison of tubulin and Eg5 dynamics in spindles by fluorescent speckle microscopy.** (a) Fluorescent speckle microscopy of labeled tubulin in spindles assembled in *Xenopus* egg extracts. The highlighted region across the spindle was used for preparing the kymograph shown in panel b. The angled streaks reveal polewards microtubule movement. (c) Fluorescent speckle microscopy of labeled Eg5 in the spindle. The highlighted region was used to prepare the kymograph shown in panel d. The vertical streaks reveal static Eg5 populations in spindles. (e) The histogram shows the distribution of rates of polewards movement of tubulin and Eg5 speckles. Videos relating to this figure are available at http://www.jcb.org/content/vol154/issue6. Bars, 5 μm.

unlabeled versions of our expressed Eg5 appear to be native and functional by several criteria. After the labeling reaction, total Eg5 protein (OD_{280}) and protein-attached fluorochrome (OD_{585}) coeluted in a sharp, symmetrical peak

within the included volume of a gel filtration column (Fig. 1 a). Unlabeled, expressed Eg5 also eluted at the same position (not shown). Calibration of the column showed that this position corresponds to a Stokes radius of 13.5 nm, as expected for Eg5 tetramer (Sharp et al., 1999). These data show that both labeled and unlabeled expressed Eg5 behaved as a monodisperse population of tetramers. The labeled Eg5 drove microtubule gliding in vitro at velocities similar to that of unlabeled full-length protein (Fig. 1 c) and that of an Eg5 fragment described previously (Mayer et al., 1999). Labeled full length Eg5 localized to spindles assembled in cell-free extracts (Figs. 1 d and 2 c) (Desai et al., 1999), with a distribution indistinguishable from that reported for the endogenous protein (Sawin et al., 1992; Kapoor et al., 2000). The motor is present throughout the spindle, but enriched towards the poles relative to microtubules (see Fig. 7 a). Under different conditions reported in this paper, added, labeled Eg5 (detected by the fluor) and endogenous Eg5 (detected by immunofluorescence) had indistinguishable localizations. Addition of 200–250 nM of unlabeled recombinant Eg5, higher than the concentrations used in our probe experiments, did not affect spindle assembly or microtubule dynamics as judged by speckle imaging of labeled tubulin (Fig. 2 a). Finally, addition of full-length recombinant protein to Eg5-depleted extracts rescued the formation of bipolar spindles (see Online supplemental material, available at http://www.jcb.org/content/vol154/issue6).

Fluorescent speckle microscopy reveals populations of static Eg5 in bipolar spindles while microtubules flux polewards

Time-lapse fluorescent speckle microscopy at 1 frame/s of mitotic extracts, to which labeled tubulin had been added, allowed observations of microtubule speckles that were correlated over many image frames (Fig. 2 a). Essentially, all tubulin speckles moved continuously polewards, as reported (Sawin and Mitchison, 1991; Waterman-Storer et al., 1998). This movement can be conveniently visualized and measured in kymographs (Fig. 2 b). Compared with published data (Sawin and Mitchison, 1991; Waterman-Storer et al., 1998), we detected more heterogeneity in the rates of polewards microtubule flux due to the high spatial and temporal resolution of our experiment (Fig. 2 e). Slower moving speckles tended to be near the pole, whereas in the center of the spindle essentially all speckles moved at near peak rates (Fig. 2 b).

We next used fluorescent speckle microscopy to examine the dynamics of Eg5 in spindles. The concentration of endogenous Eg5 in *Xenopus* egg extracts measured by Western blotting with expressed Eg5 as standard was ~400 nM (not shown, calculated for monomer). Addition of 100–150 nM of the labeled protein gave images with good speckle contrast (Fig. 2 c). Kymographs revealed streaks of Eg5 speckles normal to the spindle axis, indicating static populations of Eg5 (Fig. 2 d). These streaks of stationary Eg5 were observed throughout the spindle, and were typically 5–30 s in duration.

Comparison of the Eg5 and tubulin speckles in spindles revealed two major differences in their dynamic behavior (Fig. 2 e). First, most Eg5 speckles were static relative to the
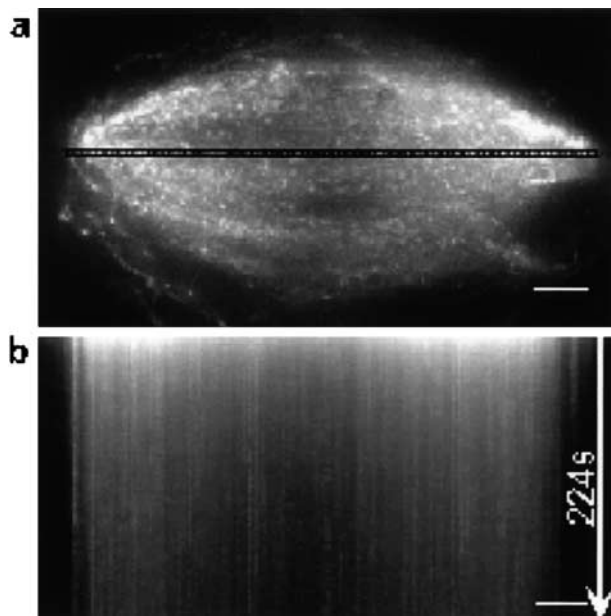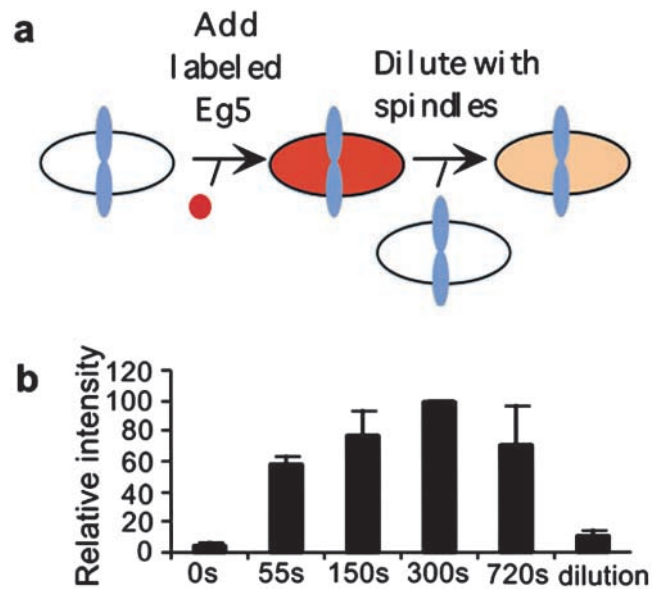
Figure 3. **Persistence of Eg5 speckles in spindles is sensitive to a nonhydrolyzable ATP analogue, AMPPNP.** (a) The distribution of labeled Eg5 in a bipolar spindle in the presence of 1.5 mM AMPPNP. The highlighted region was used to prepare the kymograph shown in panel b. The vertical streaks correspond to stationary speckles, almost all of which persist for >200 s. Bars, 5 μm.

Figure 4. **Eg5 exchanges between spindles and the bulk cytoplasm with a half-life <55 s.** (a) A schematic of a pulse-chase experiment to examine the bulk turnover of Eg5 in in vitro spindles. (b) Labeled tubulin was incorporated into spindles assembled in cell-free extract. Texas red–labeled Eg5 was added and after fixed timepoints samples were removed and diluted into fix. The ratio of Eg5 signal in spindles to that of labeled tubulin at each time point after Eg5 addition was determined. Data from three independent experiments is shown. Note saturation labeling by 300 s. Spindle-associated, labeled Eg5 can be diluted away when spindles to which labeled Eg5 has been added to saturation are mixed with 5 vol of unlabeled spindles. The ratio of labeled Eg5 to labeled tubulin, 300 s after mixing spindles with and without labeled Eg5, is shown in the column labeled "dilution".

spindle poles. 70% of the speckles analyzed moved polewards at rates less the 0.25 μm/min. Most of the microtubules in the spindle flux polewards at rates >1.1 μm/min. Thus, populations of Eg5 are static while the microtubules move polewards. Second, the persistence of Eg5 speckles in spindles is less than that observed for tubulin speckles, as reflected by the lengths of the streaks in the kymographs, suggesting a faster turnover of Eg5 than tubulin.

Eg5's ATPase cycle influences its dynamic behavior in spindles

We next examined whether the dynamic behavior of Eg5 in the spindle depended on its ATPase activity. Adenylimidodiphosphate (AMPPNP),* a nonhydrolyzable ATP analogue, inhibits kinesins in a microtubule-bound state. 1.5 mM AMPPNP was added to spindles equilibrated with labeled Eg5 and immediately prepared for fluorescent speckle microscopy (Fig. 3 a). This concentration of AMPPNP is known to promote rigor binding of Eg5 to microtubules (unpublished data) and to block polewards flux and slow microtubule turnover in *Xenopus* extract spindles (Sawin and Mitchison, 1991, 1994; Waterman-Storer et al., 1998). Eg5 speckle kymographs in AMPPNP show vertical streaks of stationary Eg5 speckles that persist for over 200 s (Fig. 3 b). The same is true for tubulin speckle kymographs (Waterman-Storer et al., 1998). This is consistent with our Eg5 probe being a functional kinesin capable of coupling ATP hydrolysis to its microtubule association. This also suggests that the dynamic association of labeled Eg5 with microtu-

bules we observed in normal spindles depends on ATPase activity of Eg5.

Eg5 can exchange between spindles and bulk cytoplasm on a time scale of seconds

Speckle persistence is difficult to quantitate, and it does not distinguish between bulk turnover (Eg5 entering or leaving a spindle) and diffusion (Eg5 moving locally on a time scale of seconds and a distance scale of microns). To measure bulk turnover of Eg5, we used a pulse-chase protocol (Fig. 4 a). Labeled Eg5 was added to an extract containing assembled spindles, and samples were removed at timepoints and fixed for quantitation of Eg5 incorporation into spindles. Added Eg5 incorporated rapidly, and its distribution was similar at all time points. Greater than 50% of steady state level of Eg5 was incorporated in 55 s (Fig. 4 b). Mixing spindles labeled to steady state with Eg5 with spindles to which no labeled Eg5 has been added lead to rapid dilution of the label, again consistent with the fast turnover of Eg5 in spindles. The mechanics of mixing the viscous extracts limits the time resolution of this experiment. We estimate a bulk turnover half-life of <55 s, consistent with the lengths of streaks in Eg5 speckles in kymographs that were typically <30 s. Both measurements indicate that Eg5 turnover is faster than that of tubulin in *Xenopus* extract spindles ($t_{1/2}$ ~100 s; Sawin and Mitchi-

---

*Abbreviation used in this paper: AMPPNP, adenylimidodiphosphate.
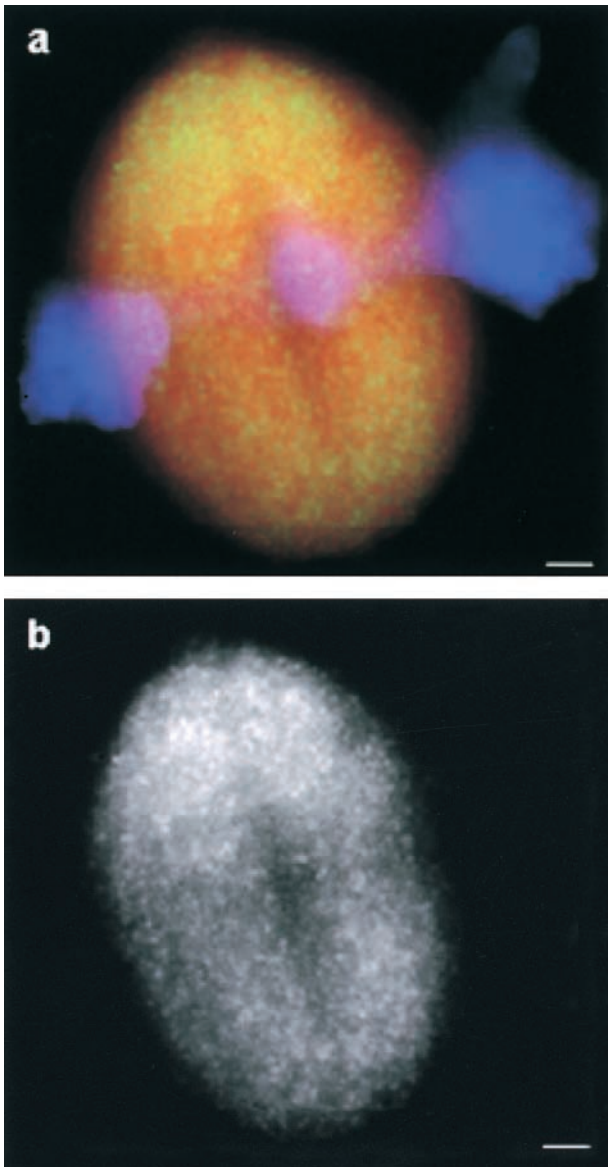
Figure 5.   **Inhibition of Eg5 motility does not accumulate the motor at spindle poles.** (a) 100 μM monastrol was added to assembled bipolar spindles and a thin (~10-μm thick) sample was prepared for microscopy. An overlay showing the distribution of labeled Eg5 (green), tubulin (red), and DNA (blue) in a bipolar spindle 15 min after monastrol addition. (b) Eg5 alone. Linescans comparing the distribution of Eg5 and tubulin in this spindle are shown in Fig. 7 b. Bars, 5 μm.

son, 1991). The bulk turnover data also have implications for Eg5 diffusion in extracts. Since Eg5 can move in and out of spindles, a distance of microns, on a time scale of seconds, it must be able to diffuse relatively quickly when not temporarily immobilized in spindles.

The distribution of Eg5 in spindles does not depend on its motility, but does depend on dynactin function

In an effort to deepen our understanding of the factors involved in Eg5 targeting to, and temporary immobilization in, spindles, we performed two types of perturbation experiments. First we treated spindles with monastrol, a small

molecule inhibitor of Eg5 motility (Mayer et al., 1999). Monastrol induces the collapse of *Xenopus* extract spindles that are not immobilized (Kapoor et al., 2000). This collapse can be inhibited by making a thin (~10 μm) squash of extract between a slide and coverslip. This preparation physically traps the spindles, and many of these "pinned" spindles retain constant length in monastrol. 100 μM monastrol does not inhibit polewards microtubule flux in pinned, bipolar spindles (Kapoor, T.M., A. Desai, P. Maddox, E.D. Salmon, and T.J. Mitchison, personal communication). Continued flux under conditions where Eg5 is inhibited by monastrol is not unexpected, since apparently normal flux was observed in rare bipolar spindles that assembled in extracts from which Eg5 had been immunodepleted (Sawin and Mitchison, 1994). This is also consistent with monastrol not inducing the formation of Eg5–microtubule rigor complexes, since the formation of these complexes could inhibit microtubule transport. The distribution of labeled Eg5 in monastrol-treated, pinned spindles (Fig. 5, b and c) was similar to control spindles (see Fig. 7 b). This experiment suggests that normal motility of Eg5 is not central to the mechanisms that target it to spindles, or immobilize it to generate speckles. Further interpretation of this experiment must await detailed characterization of the consequence of monastrol binding to Eg5 for Eg5–microtubule interactions.

Second, we assembled spindles in the presence of p50 dynamitin, which leads to the disruption of the dynactin complex and the formation of spindles with abnormally splayed poles and reduced microtubule density (Echeverri et al., 1996; Heald et al., 1997). p50 treatment does not alter microtubule polarity (Merdes et al., 2000) or block polewards flux in *Xenopus* extract spindles (Kapoor, T.M., A. Desai, P. Maddox, E.D. Salmon, T.J. Mitchison, personal communication). In p50-treated spindles, the distribution of endogenous Eg5 (Fig. 6, a and b) detected by immunofluorescence and added labeled Eg5 (Fig. 6, c and d) was severely redistributed relative to microtubules (Fig. 7 c), becoming enriched in the center of the spindle and depleted at the poles. These data suggest a role for dynactin/dynein in positioning Eg5 in spindles. The similar distribution of the Eg5 probe and endogenous Eg5 in perturbed and unperturbed spindles suggests that the labeled recombinant Eg5 is a faithful reporter for the localization of endogenous Eg5.

Discussion

Fluorescence speckle microscopy allowed comparison of Eg5 and tubulin dynamics in spindles, but what exactly were we imaging? Unlike well-characterized tubulin speckles (Waterman-Storer and Salmon, 1998) we do not know the exact physical basis for the speckled appearance of labeled Eg5 added to spindles. Under our speckling conditions ~1 Eg5 polypeptide in 8 is labeled, and in standard widefield microscopy ~2–7 fluorochromes are typically required within a single resolvable voxel (ca 0.27 × 0.27 × 1 μm) to generate an easily observed speckle (Waterman-Storer and Salmon, 1999). Thus, we suspect we are not imaging individual Eg5 tetramers, but rather several tetramers that lie within a single resolvable voxel. We do not know whether multiple tetramers must physically interact with each other

Figure 6. **Eg5 distribution in spindles depends on dynactin function.** (a) An overlay showing the immunolocalization of endogenous Eg5 (green), tubulin (red), and DNA (blue) in spindles assembled in the presence of p50 dynamitin (0.7 mg/ml), an inhibitor of dynactin. (b) Eg5 alone. (c) An overlay showing the distribution of recombinant labeled Eg5 (green), tubulin, and DNA in spindles assembled in the presence of the dynactin inhibitor. (d) Labeled Eg5 alone. Linescans comparing the distribution of Eg5 and tubulin in spindles assembled in the presence of p50 dynamitin are shown in Fig. 7 c.
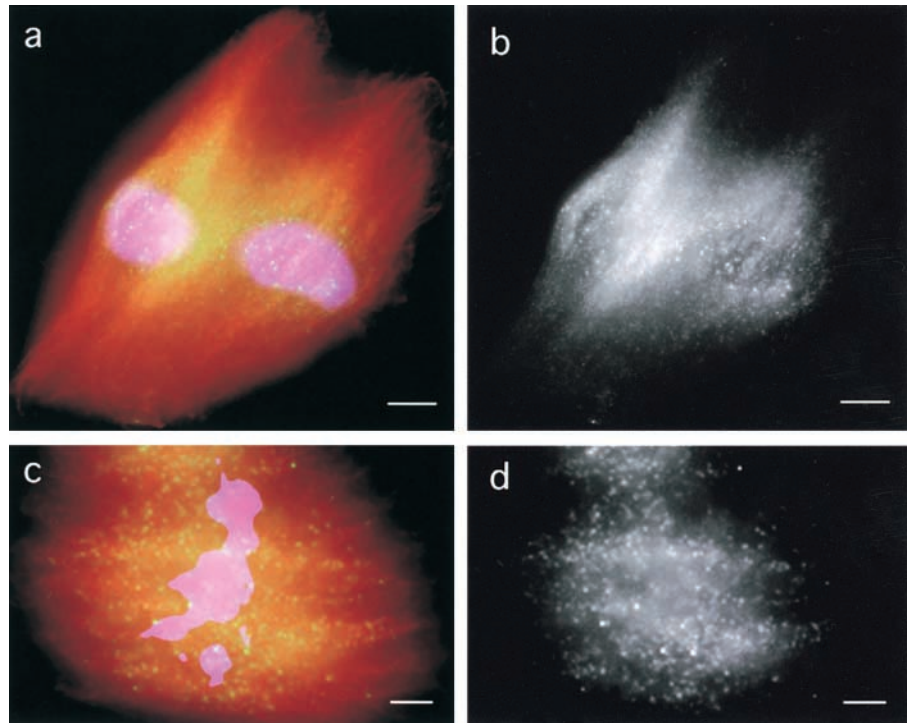
to generate a speckle, or if they can be immobilized independently. Answering this question will be an important step towards understanding the Eg5-targeting mechanism. We are confident the speckles are not a labeling artifact, but rather report on normal Eg5 dynamics for the reasons listed in the results section.

We note a possible discrepancy between our results and a recent paper in which Eg5 dynamics were probed in microtubule asters induced by an allele of the GTPase, Ran (Wilde et al., 2001). In that paper, low concentrations of a fluorescently labeled antibody raised to the stalk domain of Eg5 were added to the extract to probe Eg5 dynamics. Speckles were observed, and a fraction of them moved towards the plus end of microtubules at ~2.8 μm/min. In contrast, we observed essentially no movement of directly labeled Eg5 away from poles in regions near the poles of bipolar spindles. The difference may be due simply to differences in the behavior of Eg5 in bipolar spindles and Ran asters. It is not known if microtubules in Ran asters flux towards the center of the aster. It is also possible that the antibody technique may not provide a nonperturbing probe of Eg5 dynamics. Although the labeled antibody did not inhibit bipolar spindle formation at the low concentrations used for fluorescent speckle microscopy, antibodies to the same region of Eg5 are known to induce spindle collapse when added at higher concentrations (Sawin et al., 1992). It is possible that antistalk antibodies could induce dissociation of Eg5 tetramers from a binding site in spindles, and thus induce artificial plus end–directed motility of those Eg5 tetramers to which the antibody has bound. Analysis of antibody speckles in bipolar spindles and directly labeled Eg5 in Ran asters could help address these differences.

Our principle result is the observation of populations of Eg5 in spindles that are static during intervals over which microtubules move detectably poleward. We believe that

this observation has important implications for the mechanism of Eg5 targeting to spindles, and by extension, for more general issues of spindle organization and Eg5 function. We considered four possible explanations for immobilization of Eg5 in spindles. First, Eg5 might be free in spindles, but exhibit limited diffusion due simply to high local viscosity or viscoelasticity. We think this unlikely for several reasons. Using the Einstein-Stokes equation, we estimate that spindle viscosity would have to be >70 Poise to keep individual Eg5 tetramers (Stokes radius of 13.5 nm) within regions resolvable by light microscopy (300 nm^2) for 20 s (Alexander and Rieder, 1991). The maximum published estimate for spindle viscosity is 20-fold lower (Alexander and Rieder, 1991). Our observation that Eg5 can exhibit bulk exchange in and out of spindles over a distance of microns, on a time scale of seconds, argues against a purely viscoelastic mechanism for immobilization. Finally the density of microtubules in spindles with micron scale gaps between bundles is insufficient to act as a sieve for molecules the size of Eg5. We believe that the combined speckle and bulk turnover are better fit by a model in which Eg5 interacts transiently with some scaffold that causes it to be immobilized, but it diffuses freely when not interacting with this scaffold.

Second, individual Eg5 tetramers might walk, using their motor activity, towards the plus ends of microtubules at exactly the rate that the microtubules flux polewards. This could result in walking in place, as on a treadmill. This interpretation is complicated by the fact that microtubule orientation varies across the spindle (uniform polarity near the poles, mixed polarity near the center), and we found that Eg5 is equally immobile all over the spindle. If this interpretation were correct, Eg5 distribution in spindles would be very sensitive to inhibition of its motor function. Our monastrol data (Fig. 5) shows this is not the case, so we disfavor this interpretation.

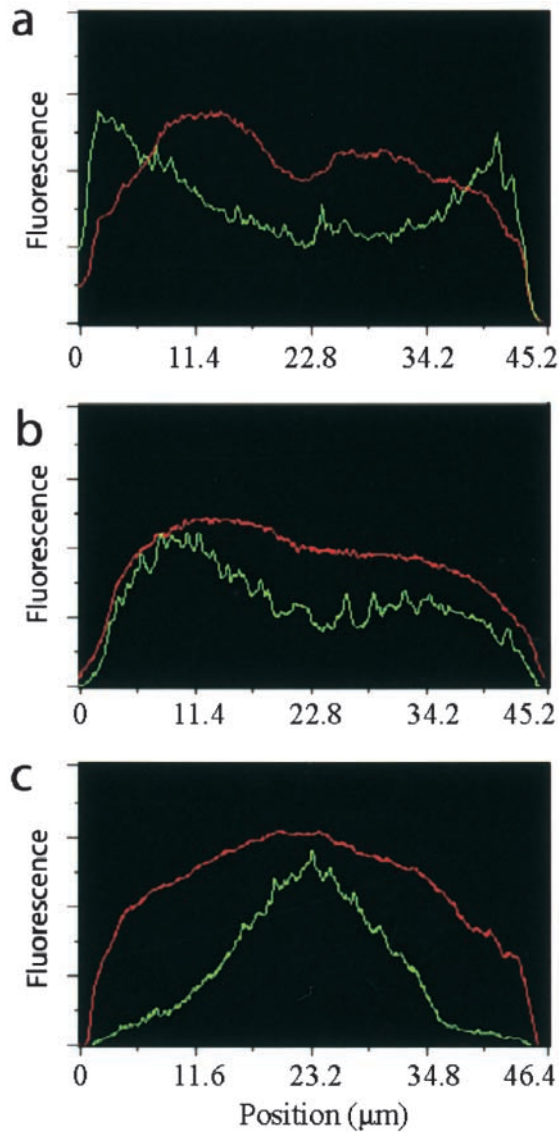Third, Eg5 might associate with a subset of microtubules

Figure 7.   **Distribution of Eg5 (green trace) relative to microtubules (red trace) in perturbed and unperturbed spindles.** (a) Linescan of fluorescence intensity (arbitrary units) across the control bipolar spindle shown in Fig. 1 d. (b) Linescan across the spindle shown in Fig. 5 showing the distribution of Eg5 in the presence of 100 µM monastrol. (c) Linescan across a bipolar spindle assembled in the presence of p50 dynamitin (Fig. 6).
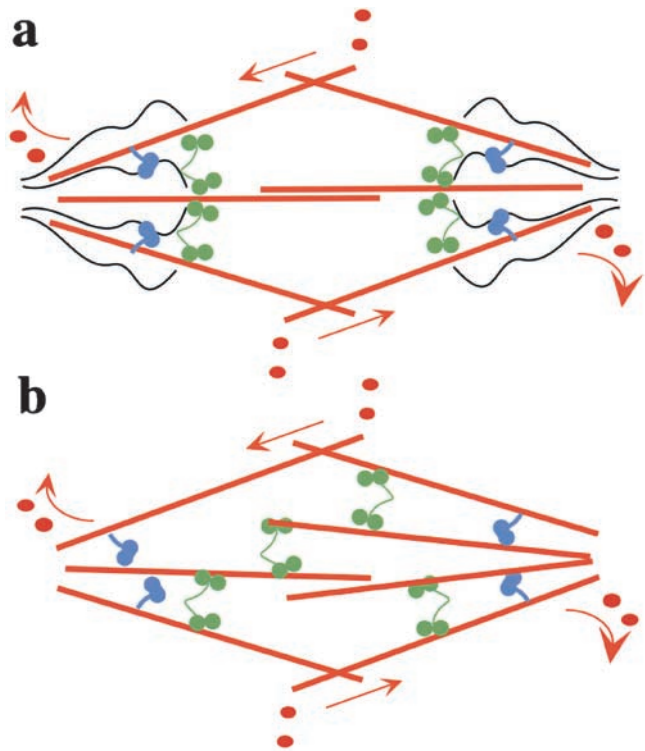

Figure 8.   **Two models for the spindle.** (a) Eg5 (green). Other motor proteins, including dynein/dynactin (blue), that interact with a static matrix (black) and microtubules (red) that are fluxing polewards (arrows). The nonmicrotubule mechanical ensemble may be an organized structure (black), whose assembly and maintenance can depend on spindle microtubules, or it may be an aspect of spindle cytoarchitecture. (b) A model for the spindle where motors, including Eg5, interact with microtubules alone. These motors crosslink and generate forces against microtubules that flux polewards.

that are not moving. Both photoactivation of fluorescence (Sawin and Mitchison, 1991) and speckle imaging (Fig. 2, a and e) suggest that the great majority of microtubules in *Xenopus* spindles are moving polewards. Both methods are biased towards observing flux in more stable microtubules, and it is possible that very recently polymerized microtubules, or a subset of unusually dynamic microtubules, are not fluxing. We did observe occasional tubulin speckles that moved poleward slowly ($\sim$0.25 µm/min), and these tended to be clustered towards the pole, where recently polymerized microtubules may be enriched. The pole is also enriched in microtubule segments aligned in part along the z axis (perpendicular to the image plane), which would slow apparent movement rates along the x, y axis. Again, the observation

that Eg5 was equally static all over the spindle argues against differential association with nonfluxing microtubules near poles. Since there is no evidence that Eg5 selectively associates with subsets of microtubules, and no definite evidence for a static subset, we disfavor this interpretation.

Although we cannot rule out the three preceding interpretations, we favor a fourth, that Eg5 physically interacts with some static, nonmicrotubule spindle component that we postulate corresponds to the hypothetical spindle matrix (Fig. 8 a). Our data provide few clues as to the identity of this hypothetical matrix. We do not think actin is involved, since spindle organization and dynamics in *Xenopus* extracts are not affected by cytochalasin D (which was present in all our experiments). We have not detected a high-affinity interaction between Eg5 and other spindle proteins, but two specific interactions are worth considering, Eg5–dynactin and Eg5–Eg5. Two-hybrid data revealed that Eg5 may physically interact with the dynein-targeting complex dynactin (Blangy et al., 1997), and we found that disruption of dynactin with p50 caused relocalization of Eg5. However, disruption of dynactin did not block targeting of Eg5 to spindles. Understanding the nature of the Eg5–dynactin interaction requires more data. We currently suspect that dynactin influences Eg5 localization indirectly, for example through positioning an unknown matrix element (Fig. 8 a). Reversible polymerization of Eg5 tetramers in the spindle to form dynamic

higher order complexes or filaments with reduced diffusion could also account for much of our data. Beyond dynactin and Eg5, we can only speculate as to the biochemical nature of a putative static spindle matrix. It might contain spindle-specific proteins such as NuMA (Dionne et al., 1999), TPX2 (Wittmann et al., 2000), or homologues of the *Drosophila* protein, Skeletor (Walker et al., 2000). It could also contain, or be made of, proteins that permeate the whole cytoplasm as well as the spindle or membrane systems. It could bind Eg5 directly, or perhaps immobilize it indirectly, by viscoelastic tethering (Seksek et al., 1997; Luby-Phelps, 2000; Papadopoulos et al., 2000). Identification of the matrix, if it exists, will require new biochemical experiments. Fluorescent speckle microscopy provides a tool to probe the dynamics of new spindle components, and thus determine if they interact primarily with fluxing microtubules or with a static matrix.

Finally, what are the implications of our data for Eg5 function? Most models posit its main function as crosslinking antiparallel, and perhaps also parallel, microtubules in the spindle, and thus promoting organization and bipolarity (Mountain et al., 1999; Sharp et al., 1999) (Fig. 8 b). An interesting question is whether Eg5 motor activity is required for this function, or merely its capability to bind to microtubules (Gheber et al., 1999). Our dynamics data do not directly address the potential crosslinking role of Eg5, but they do bring up the interesting alternative that Eg5 could organize the spindle in part by promoting microtubule–matrix interactions. A matrix with sufficient mechanical integrity to position Eg5 and hold it in place over seconds would serve as an anchor point from which Eg5, and perhaps other motors such as dynein, could organize microtubules and exert forces in the spindle (Gordon et al., 2001). As such, the matrix may be a major player in spindle mechanics, analogous to thick filaments in muscle.

Materials and methods

Labeling and expression of recombinant proteins
Full-length Eg5 with an NH_2 terminus polyhistidine tag was expressed using the Bac-to-Bac system (GIBCO BRL) in SF9 cells. 72 h after infection, the SF9 cells were harvested and the pellets were frozen in liquid nitrogen. Cell pellets were lysed (50 mM KPO_4, 250 mM KCl, 10 mM imidazole, 1 mM PMSF, 10 mM BME, 0.5 mM MgATP, 1% Igepal CA-630, protease inhibitors [10 μM leupeptin, 10 μM pepstatin A, 10 μM chymostatin], pH 8.0) and clarified (125,000 g, 45 min) and the supernatant was incubated with Ni-NTA agarose (QIAGEN) in batch for 90 min. The resin was then washed extensively with wash buffer (10% glycerol, 50 mM KPO_4, 250 mM KCl, 10 mM imidazole, 1 mM benzamidine, 10 mM BME, 0.1 mM MgATP, protease inhibitors, pH 8.0). To label the protein, the resin was washed with coupling buffer (10% glycerol, 50 mM KPO_4, 250 mM KCl, 0.1 mM MgATP, protease inhibitors, pH 8.0), followed by the addition of 100 μM Texas red X-succinimidyl ester (Molecular Probes). After 30 min at 4°C, the coupling reaction was quenched with glutamate (50 mM) for 15 min. The resin was then washed extensively (10% glycerol, 50 mM KPO_4, 250 mM KCl, 10 mM imidazole, 1 mM benzamidine, 10 mM BME, 0.1 mM MgATP, protease inhibitors, pH 6.0) and the protein was eluted (10% glycerol, 50 mM KPO_4, 150 mM KCl, 250 mM imidazole, 1 mM benzamidine, 10 mM BME, 0.1 mM MgATP, protease inhibitors, pH 7.0), dialyzed against superose buffer (10 mM Hepes, 150 mM sucrose, 250 mM KCl, 10 μM MgATP, 1 mM DTT, protease inhibitors, pH 8.0), and purified over a size exclusion column (Superose 6; Amersham Pharmacia Biotech). Concentrations of Eg5 are calculated for the monomer. The protein-labeling stoichiometry estimated by spectrophotometry was ~0.5 fluor/Eg5 molecule. Typically, the labeled protein was used within a few hours after purification, since freezing it caused aggregation. p50 dynamitin was expressed and purified as described (Wittmann and Hyman, 1999).

Monastrol was prepared as described (Mayer et al., 1999). Labeled tubulins were prepared as described (Hyman et al., 1991).

Spindle assembly in vitro
Spindles were assembled in cytostatic factor–arrested *Xenopus* laevis egg extracts cycled through interphase to replicate the DNA and centrosomes as described (Desai et al., 1999). p50 dynamitin was added with the second addition of cytostatic factor–arrested extract during spindle assembly.

Fluorescent speckle microscopy and analysis
The amount of labeled protein added to *Xenopus* egg extracts was optimized for each protein preparation. For microtubule fluorescent speckle microscopy, Texas red–labeled tubulin was used at concentrations ranging from 6 to 30 nM (0.9 fluorophores per tubulin dimer). For Eg5 fluorescent speckle microscopy, Texas red–labeled Eg5 was typically used at 100–150 nM. Samples were imaged with a 100× objective (Plan Apo, Nikon; NA 1.4) and a camera (MicroMax cooled CCD, Princeton Instruments; bin 2 × 2). Time-lapse images (400-ms exposure) were collected at 1-s intervals using a digital imaging system controlled by Metamorph software (Universal Imaging Corp.). Kymographs were prepared from unprocessed images by selecting a seven pixel wide line extending from one spindle pole to the other. In brief, a line seven pixels wide (x-dimension) was drawn across the spindle (y-dimension). The software recorded the maximum intensity pixel across the x-dimension for each point along the line (y-dimension). The finished image consists of the above measurement performed for each timepoint, placed one after another by the software to display intensity differences over time. Slopes of streaks of correlated speckles were measured to determine rates of movement relative to the spindle poles. Five spindles from four independent experiments were analyzed to determine the rates of Eg5 and tubulin speckle movements. Each spindle was divided into two halves and rates for seven speckles uniformly distributed in each half were measured relative to the corresponding spindle pole. The velocities were binned into 0.5 μm/min increments to generate velocity distribution histograms.

Turnover of Eg5
500 nM Alexa 488–labeled tubulin was added to spindles assembled in *Xenopus* egg extracts cycled through interphase. At the completion of assembly, Texas red–labeled Eg5 was added to the extracts (140 nM) and samples were removed at different time points, diluted, and fixed (7.5% formaldehyde). The samples were imaged using a Nikon 40× Plan Fluor objective (NA 0.75) and a Princeton Instruments MicroMax cooled CCD camera. The ratio of the average intensities of the Texas red signal and the Alexa fluor signal (both corrected for sample background) was determined for five spindles for each time point. The data for each experiment was normalized to the ratio at the 300 s time point. Averages of three independent experiments are shown with SD. For the "dilution" experiment, spindles in extract with labeled Eg5 incorporated to saturation and labeled tubulin were mixed with 5 vol of extracts with assembled spindles, labeled tubulin, and no labeled Eg5. After 5 min, samples were fixed and processed for imaging.

Linescans
Linescans were generated using functions in Metamorph software (Univeral Imaging Corp.). The average intensity over a 10 pixel wide region draw across the unprocessed image is calculated for each channel of fluorescence by the software. Regions selected for linescans extended through the center of the perturbed or control spindle images, parallel to the long axis of the structure. Overlays of pseudocolored graphs were prepared using Adobe Photoshop® 6.0.

Viscosity calculation
The Einstein-Stokes equation was used to determine the viscosity of the spindle with time (t) = 20 s, temperature (T) = 300 K, mean free path (X) = 300 nm, Stokes radius (a) = 13.5 nm, and k = Boltzman constant (viscosity = $kTt/3\pi aX^2$).

Online supplemental material
Data for immunodepletion and rescue by add-back of recombinant Eg5 is provided. Time-lapse videos corresponding to spindles shown in Fig. 2 and additional videos for Eg5 and microtubule fluorescent speckle microscopy are also provided. The videos are available at http://www.jcb.org/content/vol154/issue6.

References

Alexander, S.P., and C.L. Rieder. 1991. Chromosome motion during attachment to the vertebrate spindle: initial saltatory-like behavior of chromosomes and quantitative analysis of force production by nascent kinetochore fibers. *J. Cell Biol*. 113:805–815.

Blangy, A., H.A. Lane, P. d'Herin, M. Harper, M. Kress, and E.A. Nigg. 1995. Phosphorylation by p34cdc2 regulates spindle association of human Eg5, a kinesin-related motor essential for bipolar spindle formation in vivo. *Cell*. 83:1159–1169.

Blangy, A., L. Arnaud, and E.A. Nigg. 1997. Phosphorylation by p34cdc2 protein kinase regulates binding of the kinesin-related motor HsEg5 to the dynactin subunit p150. *J. Biol. Chem*. 272:19418–19424.

Desai, A., A. Murray, T.J. Mitchison, and C.E. Walczak. 1999. The use of *Xenopus* egg extracts to study mitotic spindle assembly and function in vitro. *Methods Cell Biol*. 61:385–412.

Dionne, M.A., L. Howard, and D.A. Compton. 1999. NuMA is a component of an insoluble matrix at mitotic spindle poles. *Cell Motil. Cytoskeleton*. 42:189–203.

Echeverri, C.J., B.M. Paschal, K.T. Vaughan, and R.B. Vallee. 1996. Molecular characterization of the 50-kD subunit of dynactin reveals function for the complex in chromosome alignment and spindle organization during mitosis. *J. Cell Biol*. 132:617–633.

Enos, A.P., and N.R. Morris. 1990. Mutation of a gene that encodes a kinesin-like protein blocks nuclear division in *A. nidulans. Cell*. 60:1019–1027.

Forer, A., T. Spurck, and J. Pickett-Heaps. 1997. Ultraviolet microbeam irradiation of spindle fibres in crane-fly spermatocytes and newt epithelial cells: resolution of previously conflicting observations. *Protoplasma*. 197:230–240.

Gheber, L., S.C. Kuo, and M.A. Hoyt. 1999. Motile properties of the kinesin-related Cin8p spindle motor extracted from *Saccharomyces cerevisiae* cells. *J. Biol. Chem*. 274:9564–9572.

Gordon, M., L. Howard, and D. Compton. 2001. Chromosome movement in mitosis requires microtubule anchorage at spindle poles. *J. Cell Biol*. 152:425–434.

Hagan, I., and M. Yanagida. 1990. Novel potential mitotic motor protein encoded by the fission yeast cut7+ gene. *Nature*. 347:563–566.

Heald, R., R. Tournebize, A. Habermann, E. Karsenti, and A. Hyman. 1997. Spindle assembly in *Xenopus* egg extracts: respective roles of centrosomes and microtubule self-organization. *J. Cell Biol*. 138:615–628.

Heck, M.M., A. Pereira, P. Pesavento, Y. Yannoni, A.C. Spradling, and L.S. Goldstein. 1993. The kinesin-like protein KLP61F is essential for mitosis in *Drosophila. J. Cell Biol*. 123:665–679.

Hoyt, M.A., L. He, K.K. Loo, and W.S. Saunders. 1992. Two *Saccharomyces cerevisiae* kinesin-related gene products required for mitotic spindle assembly. *J. Cell Biol*. 118:109–120.

Hyman, A., D. Drechsel, D. Kellogg, S. Salser, K. Sawin, P. Steffen, L. Wordeman, and T. Mitchison. 1991. Preparation of modified tubulins. *Methods Enzymol*. 196:478–485.

Inoue, S., and E.D. Salmon. 1995. Force generation by microtubule assembly/disassembly in mitosis and related movements. *Mol. Biol. Cell*. 6:1619–1640.

Kapoor, T.M., T.U. Mayer, M.L. Coughlin, and T.J. Mitchison. 2000. Probing spindle assembly mechanisms with monastrol, a small molecule inhibitor of the mitotic kinesin, Eg5. *J. Cell Biol*. 150:975–988.

Leslie, R.J., R.B. Hird, L. Wilson, J.R. McIntosh, and J.M. Scholey. 1987. Kinesin is associated with a nonmicrotubule component of sea urchin mitotic spindles. *Proc. Natl. Acad. Sci. USA*. 84:2771–2775.

Luby-Phelps, K. 2000. Cytoarchitecture and physical properties of cytoplasm: volume, viscosity, diffusion, intracellular surface area. *Int. Rev. Cytol*. 192:189–221.

Maddox, P.S., K.S. Bloom, and E.D. Salmon. 2000. The polarity and dynamics of microtubule assembly in the budding yeast *Saccharomyces cerevisiae. Nat. Cell Biol*. 2:36–41.

Mayer, T.U., T.M. Kapoor, S.J. Haggarty, R.W. King, S.L. Schreiber, and T.J. Mitchison. 1999. Small molecule inhibitor of mitotic spindle bipolarity identified in a phenotype-based screen. *Science*. 286:971–974.

Mazia, D. 1961. Mitosis and the physiology of Cell Division. *In* The Cell. Biochemistry, Physiology and Morphology. J. Brachvhet and A.C. Mirsky, editors. Academic Press, NY. 61–412.

McIntosh, J.R., P.K. Hepler, and D.G. Van Wie. 1969. Model for mitosis. *Nature*. 224:659–663.

Merdes, A., R. Heald, K. Samejima, W.C. Earnshaw, and D.W. Cleveland. 2000. Formation of spindle poles by dynein/dynactin-dependent transport of NuMA. *J. Cell Biol*. 149:851–862.

Mitchison, T.J. 1989. Polewards microtubule flux in the mitotic spindle: evidence from photoactivation of fluorescence. *J. Cell Biol*. 109:637–652.

Mitchison, T., and M. Kirschner. 1984. Dynamic instability of microtubule growth. *Nature*. 312:237–242.

Mountain, V., C. Simerly, L. Howard, A. Ando, G. Schatten, and D.A. Compton. 1999. The kinesin-related protein, HSET, opposes the activity of Eg5 and cross-links microtubules in the mammalian mitotic spindle. *J. Cell Biol*. 147:351–366.

Nicklas, R.B. 1988. The forces that move chromosomes in mitosis. *Annu. Rev. Biophys. Biophys. Chem*. 17:431–449.

Papadopoulos, S., K.D. Jurgens, and G. Gros. 2000. Protein diffusion in living skeletal muscle fibers: dependence on protein size, fiber type, and contraction. *Biophys. J*. 79:2084–2094.

Pickett-Heaps, J.D., D.H. Tippit, and K.R. Porter. 1982. Rethinking mitosis. *Cell*. 29:729–744.

Pickett-Heaps, J., T. Spurck, and D. Tippit. 1984. Chromosome motion and the spindle matrix. *J. Cell Biol*. 99:137s–143s.

Salmon, E.D., and R.R. Segall. 1980. Calcium-labile mitotic spindles isolated from sea urchin eggs (Lytechinus variegatus). *J. Cell Biol*. 86:355–365.

Sawin, K.E., and T.J. Mitchison. 1991. Poleward microtubule flux mitotic spindles assembled in vitro. *J. Cell Biol*. 112:941–954.

Sawin, K.E., and T.J. Mitchison. 1994. Microtubule flux in mitosis is independent of chromosomes, centrosomes, and antiparallel microtubules. *Mol. Biol. Cell*. 5:217–226.

Sawin, K.E., and T.J. Mitchison. 1995. Mutations in the kinesin-like protein Eg5 disrupting localization to the mitotic spindle. *Proc. Natl. Acad. Sci. USA*. 92:4289–4293.

Sawin, K.E., K. LeGuellec, M. Philippe, and T.J. Mitchison. 1992. Mitotic spindle organization by a plus-end-directed microtubule motor. *Nature*. 359:540–543.

Schnackenberg, B.J., A. Khodjakov, C.L. Rieder, and R.E. Palazzo. 1998. The disassembly and reassembly of functional centrosomes in vitro. *Proc. Natl. Acad. Sci. USA*. 95:9295–9300.

Seksek, O., J. Biwersi, and A.S. Verkman. 1997. Translational diffusion of macromolecule-sized solutes in cytoplasm and nucleus. *J. Cell Biol*. 138:131–142.

Sharp, D.J., K.L. McDonald, H.M. Brown, H.J. Matthies, C. Walczak, R.D. Vale, T.J. Mitchison, and J.M. Scholey. 1999. The bipolar kinesin, KLP61F, cross-links microtubules within interpolar microtubule bundles of *Drosophila* embryonic mitotic spindles. *J. Cell Biol*. 144:125–138.

Sharp, D.J., G.C. Rogers, and J.M. Scholey. 2000. Microtubule motors in mitosis. *Nature*. 407:41–47.

Walker, D.L., D. Wang, Y. Jin, U. Rath, Y. Wang, J. Johansen, and K.M. Johansen. 2000. Skeletor, a novel chromosomal protein that redistributes during mitosis provides evidence for the formation of a spindle matrix. *J. Cell Biol*. 151:1401–1412.

Waterman-Storer, C.M., and E.D. Salmon. 1998. How microtubules get fluorescent speckles. *Biophys. J*. 75:2059–2069.

Waterman-Storer, C.M., and E.D. Salmon. 1999. Fluorescent speckle microscopy of microtubules: how low can you go? *FASEB J*. 13:S225–S230.

Waterman-Storer, C.M., A. Desai, J.C. Bulinski, and E.D. Salmon. 1998. Fluorescent speckle microscopy, a method to visualize the dynamics of protein assemblies in living cells. *Curr. Biol*. 8:1227–1230.

Wilde, A., S.B. Lizarraga, L. Zhang, C. Wiese, N.R. Gliksman, C.E. Walczak, and Y. Zheng. 2001. Ran stimulates spindle assembly by altering microtubule dynamics and the balance of motor activities. *Nat. Cell Biol*. 3:221–227.

Wittmann, T., and T. Hyman. 1999. Recombinant p50/dynamitin as a tool to examine the role of dynactin in intracellular processes. *Methods Cell Biol*. 61:137–143.

Wittmann, T., M. Wilm, E. Karsenti, and I. Vernos. 2000. TPX2, A novel *Xenopus* MAP involved in spindle pole organization. *J. Cell Biol*. 149:1405–1418.

Wittmann, T., A. Hyman, and A. Desai. 2001. The spindle: a dynamic assembly of microtubules and motors. *Nat. Cell Biol*. 3:E28–E34.